Chemistry of Heterocyclic Compounds, Vol.35, No. 7, 1999

REACTIVITY AND ELECTRONIC STRUCTURE OF THE GROUND AND EXCITED STATES OF OXAZOLE, 2-PHENYLOXAZOLE, AND 2-PHENYLTHIAZOLE

A. E. Obukhov and L. I. Belen'kii

The relationship of the electronic structure of oxazole, 2-phenyloxazole, and 2-phenylthiazole to the properties of the electronic excited states and transitions is examined. Spectral properties of these compounds in the free state (no effect from external perturbations) and in complexes with the proton and aprotic acids are measured and calculated by quantum-chemical PPP/S (π-approximation) and INDO/S (sp-basis) methods. Features of the electronic excitation of the atoms and the vibronic interaction of bonds in the singlet and triplet states are examined for a change of the various structural forms of azoles, which determine their spectral fluorescence properties and reactivity. Possible direction control of reactions and optimized syntheses of new compounds with given properties are discussed based on a study of the properties of the ground and excited states.

The physical and chemical properties of organic luminophores that are broadly utilized in scientific and industrial applications (in particular, the fabrication of active elements for dye lasers, information systems, nanotechnology, photodynamic therapy of cancer, pharmacology, criminalistics, etc.) are widely studied in order to elucidate the structure of polyatomic quantum systems and their excited electronic states (in this context the molecules are considered to transform energy from various types of excitation sources into light) [1-6]. A large database on organic luminophores is now available [2]. However, new compounds with various photophysical properties are continuously synthesized. Quantum-chemical methods play an integral role in evaluating these compounds and the most fruitful ways of modifying them [7].

The structure of a crystalline organic compound can be determined using X-ray methods [8]. However, new organic molecules are usually synthesized in solution at various temperatures and pH values [9-14], i.e., under conditions where diffraction methods do not provide the required information about such molecular parameters as the bond angles and lengths. Nevertheless, compounds with useful properties need to be synthesized even if they have a limited number of spectral properties. Therefore, Parizer–Parr–Pople (PPP/S, π-approximation) and intermediate neglect of differential overlap (INDO/S, *sp*-basis) quantum-chemical semi-empirical methods [9, 15-19] are used to elucidate the dependence between the structure of complicated molecules and the properties of the excited electronic states and transitions. These methods enable the interpretation of experimental data on spectral-luminescence properties such as the quantum yield and fluorescence lifetime, wavelength maxima in the fluorescence spectra, UV absorption, light emission and the 0–0 transition, the energy of the singlet and triplet levels, dipole moments, oscillator strengths of electronic transitions, and other parameters [18] as well as data on the reactivity of molecules of various electronic and geometric structures and in various environments [9-14].

Russian Peoples' Friendship University, Moscow 117302, e-mail: aobukhov@mx.pfu.edu.ru; N. D. Zelinsky Institute of Organic Chemistry, Russian Academy of Sciences, Moscow 117913, e-mail: lb@1september.ru.
Translated from Khimiya Geterotsiklicheskikh Soedinenii, No. 7, pp. 948-974, July, 1999. Original article submitted January 12, 1999.

 0009-3122/99/3507-0832$22.00

The present article is a continuation of our work [19] involving changes in the direction of electrophilic substitution and the electron-density distribution in the excited states in 2-aryl- and 2-hetaryloxazoles as a function of the nature of the substituent in the 2-position (phenyl, 2-thienyl, and 2-furyl) of the oxazole ring. In this work, the effect of changing the "pyrrole" heteroatom while keeping the substituent constant is studied. Therefore, the compounds studied are 2-phenyloxazole (PO) and 2-phenylthiazole (PT) and their complexes with proton and aprotic acids.

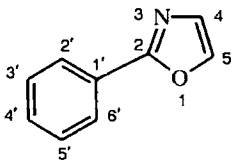

PO

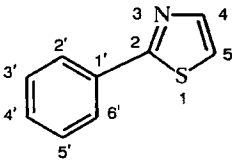

PT

It is very important that the structures and optical and magnetic properties of the molecules change regularly in the studied series: 1) a natural transition is made from mono- to bicyclic five-membered N,O- and N,S-heteroaromatic compounds, azoles; 2) a sequential replacement of the heteroatom from one with a lower atomic number to one with a higher atomic number is effected in compounds with an equal number of rings and bonding atomic and molecular orbitals. The nature of the vibronic interaction of the atomic groups in the molecules in the absence of intermolecular collisions and with changing solution pH can be studied experimentally and by quantum-chemical methods. The problem has been formulated more generally in the literature [5].

1. EXPERIMENTAL MEASUREMENTS AND CALCULATIONS

1.1. Spectral Measurements

UV absorption spectra were measured on a Specord M-40 spectrometer. The uncertainty in the position of the absorption maxima was less than 30-100 cm^{-1}. UV electronic absorption spectra were recorded in the form of the log of the molar absorption coefficient ε_{abs}^{ν} (M/l) as a linear function of frequency. This follows from the Beer–Lambert law [22]: $\varepsilon_{abs}^{\nu} = D/C_m l$, where C_m is the molar concentration, l is the absorption pathlength (cm), and D is the optical density of the solution.

Excitation and fluorescence spectra of the molecules were measured on an SLM-4800S spectrofluorometer. The measured quantum yield γ and fluorescence lifetime τ of the molecules in various solvents (relative to a solution of anthracene in ethanol, $\gamma = 0.22$ [15-18]) were used to calculate the rates of radiative decay and interconversion (k_{fl} and k_{ST}), the absorption cross section ($\sigma_{13}^{max,ads}$), and the cross section of stimulated emission (σ_{31}^{fl} or σ_{31}^{ocs}) for a trilevel model of the population equilibrium in the organic molecule [18]. The profile of the limiting amplification band χ_{31} (ν_{ocs}^{max}) was found from the experimental fluorescence spectrum, $\chi_{31}(\nu) \approx w_{fl}(\nu)/\nu^3$ [21]. Frequencies ν_{abs}^{max} and ν_{fl}^{max} in spectra of the free molecules were determined relative to that calculated by the PPP/S-CI or INDO/S-CI methods for the purely electronic 0–0 transition. As demonstrated previously [16-18], the Stokes shifts for heteroaromatic systems in the free state and in solution are very similar, i.e., they can be considered to be known from experiments with solutions. Excitation energy can be equilibrated over the vibrational states of freedom before light is emitted in a statistical ensemble of free excited complex molecules [22].

The rate constant of radiative decay and the fluorescence quantum yield are calculated using the formulas [18]:

$$k_{fl} = \gamma/\tau, \quad (1)$$

$$k_{ST} \approx (1 - \gamma)/\tau, \quad (2)$$

where γ (γ_{fl}) and τ (τ_{fl}) are the measured quantum yield and fluorescence lifetime of the molecule.

1.2. Quantum-Chemical Calculations

Semi-empirical quantum-chemical calculations were performed using the PPP/S and INDO/S methods and the spectral parameters for all possible planar conformational isomers of the molecules [23]. Thus, the PPP/S version considered at least 100 configurations (10×10 matrix); INDO/S, at least 625 (25×25). This ensured that the calculated spectral parameters were sufficiently accurate. In order to calculate the transition frequencies and intensities

$$S_0 \rightarrow S_n^*,\ S_1^* \rightarrow S_0,\ S_1^* \rightarrow S_n^*,\ T_1 \rightarrow T_n,\ T_1 \rightarrow S_0$$

in the UV absorption and fluorescence spectra and the 0–0 transition, the oscillator strength was calculated using the formula [18]:

$$f_e = 1{,}085 \cdot 10^{-5} \cdot \Delta E^*_{i\rightarrow j} \sum_{A\in\mu A}\sum |\hat{M}_\mu|^2 \Delta\rho^*_{\mu\nu}, \tag{3}$$

where $\Delta E^*_{i\rightarrow j}$ is the energy of the $S_0 \rightarrow S_n^*$ electronic transition, $T_1 \rightarrow S_0$ (cm^{-1}); M_μ is the transition dipole moment ($\hat{M}_\mu \equiv er_\mu$, r_μ is the radius vector of the μ-th electron of the A-th atom in the molecule); $\Delta\rho^*_{\mu\nu}$ is the difference matrix of the electron density for the interacting electronic states.

According to the one-electron approximation, electronic transitions between the highest-occupied (HOMO) and lowest unoccupied (LUMO) molecular orbitals (MO) in the molecules are accompanied by intramolecular charge transfer (ICT) from one subsystem to another. The magnitude and direction of the ICT are determined by the change in the electron population $\Delta\rho_{\mu\mu}^{i\rightarrow j}$ on the atoms of the subsystem [24]:

$$ICT^{i\rightarrow j}_{subsys} = \sum_{\mu\in subsys} \Delta\rho^{i\rightarrow j}_{\mu\mu}. \tag{4}$$

The contribution of each structural fragment to the overall molecular redistribution of excitation during a one-electron transition in polyatomic molecules with an uneven electron-density distribution is determined by the excitation localization expressed as the ratio of the sum of the moduli for the changes in the charge on the atoms of the fragment to the corresponding sum over all atoms of the molecule or the ratio of the sum of the moduli for the changes in the orders of the chemical bonds of any one fragment to the corresponding sum over all bonds in the molecule [24]:

$$L\mu\left(L^{i\rightarrow j}_{subsys}(\Delta\rho\mu\nu)\right) = \sum_{\mu\in subsys} |\Delta\rho^{i\rightarrow j}_{\mu\mu}| \Big/ \sum_{\mu\in molec} |\Delta\rho^{i\rightarrow j}_{\mu\mu}|. \tag{5}$$

Normalized excitation localizations on atoms ($0 \le L_\mu \le 1$) and fragments ($\Sigma_\mu L_\mu$, %) in the molecule are estimated using the formula

$$L\mu = \sum_{\nu=1}^{m}\left[D^0_{\mu\nu}\right]^2 = \sum_{\nu=1}^{m}\left[1/\sqrt{2}\sum_{i=1}^{n}\sum_{p=n+1}^{m} d_{pi}\left(C_{\mu p}\cdot C_{\nu i} + C_{\nu p}\cdot C_{\mu i}\right)\right]^2, \tag{6}$$

where the spin-free transition density matrix $[D_{\mu,\nu}^\circ]$ is formulated based on atomic orbitals (AO) of the molecular system (n is the number of occupied MO; m, the number of AO); d_{pi} is the configurational coefficients of the CI matrix, and $C_{\mu i}$ are the coefficients for AO in MO that are obtained, for example, by PPP/S-CI or INDO/S-CI methods.

Two-center two-electron integrals $\gamma_{\mu\nu}$ were calculated using the Mataga–Nishimoto formula [25]:

$$\gamma_{\mu\nu} = 1/2\ \{(\gamma_{\mu\mu} + \gamma_{\nu\nu})/[1 + 0.06944) \cdot 1/2 \cdot r_{\mu\nu}(\gamma_{\mu\mu} + \gamma_{\nu\nu})]\}, \tag{7}$$

where $r_{\mu\nu}$ is the bond length. The one-center integrals $\gamma_{\mu\mu}$ {Eq. (8) [26]} are usually set equal to the difference between the ionization potentials and electron affinities (for the 1*s*-AO of H and the 2*p*-AO of heteroatoms):

$$\gamma_{\mu\mu}(\gamma_{AA}) = I^A_p - I^B_p. \quad (8)$$

Values of the ionization potentials and the electron affinities were taken from the literature [27].

Resonance integrals $\beta_{\mu\nu}$ between the AO φ_μ (atom A) and φ_ν (atom B) are expressed as:

$$\beta_{\mu\nu} = 1/2(\beta^0_A + \beta^0_B)S_{\mu\nu}, \quad (9)$$

where $S_{\mu\nu}$ is the overlap integral and $\beta_A{}^0$ and $\beta_B{}^0$ are empirical parameters characteristic of each atom. The quantities $\beta_{\mu\nu}$ for C–C, C–N, C–O, and C–S bonds were varied during iterations as a function of the bond orders ($p_{\mu\nu}$) [28]:

$$\beta_{\mu\nu} = A_{\mu\nu} + B_{\mu\nu} \cdot p_{\mu\nu}. \quad (10)$$

The overlap integral was resolved into its σ- and π-components during its calculation by the INDO/S-CI method. The components were calculated by the usual method for Slater AO (a fitting coefficient of 0.585 is used for elements of the first to third rows of the Periodic Table) [26, 29]. Thus, Eq. (9) becomes:

$$\beta_{\mu\nu} = 1/2(\beta^0_A + \beta^0_B)(S^\sigma_{\mu\nu} + 0.585S^\pi_{\mu\nu}). \quad (11)$$

The one-center integrals of the electron kinetic energy are calculated using the formula [26]:

$$E_{kk} = 1/2(I^A_p + I^B_p) + (Z_A - 1/2)\gamma_{AA}. \quad (12)$$

Bond lengths of aromatic or heteroaromatic rings that were used in the INDO/S calculations were taken from the literature [30]. The bond angles for the benzene ring in the PPP/S-CI method were set at 120°; for the five-membered ring (furan, thiophene, oxazole), 108°. Bond lengths in each iteration were refined as a function of the bond orders [26]:

$$r_{\mu\nu} = L_{\mu\nu} + M_{\mu\nu}P_{\mu\nu}. \quad (13)$$

The integrals $\gamma_{\mu\nu}$ and $\beta_{\mu\nu}$ in addition to the bond lengths were calculated for bound atoms. For nonbonded atoms, $\beta_{\mu\nu}$ were assumed to be zero whereas $\gamma_{\mu\nu}$ remained unchanged. The methyl group was represented as an effective heteroatom. The principal results of the experiments and calculations are given in Tables 1-6 and in Figs. 1-4.

2. SPECTRAL RESULTS

2.1. Direction of Electrophilic Substitution and Reactivity in the Ground State

Our data show that the oxazole ring in 2-aryl- and 2-hetaryloxazoles behaves toward electrophiles as an activated five-membered heteroaromatic system with one heteroatom. It is brominated by bromine without a catalyst. It is nitrated by mild agents such as N-nitropicolinium tetrafluoroborate and undergoes Vilsmeier formylation [11, 12].

The direction of electrophilic substitution changes on going from free PO to the protonated form or the H-bonded complex PO–protic acid (PO–HAn) because the electron density is significantly reduced, especially in the position 5. This is clearly evident in the PMR spectra despite the requisite difference in solvents [12]. Similar effects are observed upon protonation of 2-methylthiazole (2-Me-T) and 2-phenylthiazole (PT) [31]. Complexation with $AlCl_3$ causes qualitatively the same effect as protonation of the azocycles.

TABLE 1. Reactivity Indices of Oxazole and Thiazole Compounds

Compound	Index*	$O_{(1)}$	$C_{(2)}$	$N_{(3)}$	$C_{(4)}$	$C_{(5)}$	$C_{(1')}$	$C_{(2')}$	$C_{(3')}$	$C_{(4')}$	$C_{(5')}$	$C_{(6')}$
Oxazole	FV	0.042	0.482	0.113	0.386	0.498						
	FED(E)	0.016	0.539	0.077	0.518	0.851						
	FED(N)	0.331	0.856	0.226	0.068	0.518						
	FED(R)	0.173	0.698	0.152	0.293	0.684						
2-Methyloxazole	FV	0.123	0.199	0.197	0.532	1.379						
	FED(E)	0.030	0.397	0.230	0.853	0.098						
	FED(N)	0.286	0.777	0.083	0.853	0.078						
	FED(R)	0.158	0.587	0.156	0.712	0.088						
2-Phenyloxazole	FV	0.063	0.243	0.139	0.385	0.507	0.166	0.423	0.396	0.407	0.396	0.423
	P(E)	0.021	0.310	0.139	0.277	0.581	0.165	0.133	0.019	0.205	0.032	0.117
	P(N)	0.122	0.219	0.191	0.000	0.162	0.379	0.174	0.084	0.403	0.046	0.219
	P(R)	0.071	0.265	0.165	0.139	0.372	0.272	0.154	0.052	0.304	0.039	0.168
2-Phenylthiazole	FV	0.573	0.351	0.168	0.416	0.639	0.147	0.429	0.396	0.409	0.395	0.428
	FED(E)	0.022	0.248	0.222	0.300	0.626	0.147	0.110	0.020	0.177	0.023	0.106
	FED(N)	0.044	0.458	0.305	0.035	0.291	0.190	0.171	0.033	0.268	0.023	0.183
	FED(R)	0.033	0.353	0.263	0.167	0.458	0.168	0.141	0.027	0.222	0.023	0.144
PO–HAn complex	FV	0.010	0.334	-0.821	0.520	0.509	0.147	0.433	0.396	0.411	0.395	0.430
	FED(E)	0.069	0.155	0.028	0.553	0.709	0.136	0.094	0.012	0.144	0.032	0.066
	FED(N)	0.179	0.582	0.107	0.084	0.048	0.198	0.199	0.044	0.310	0.016	0.233
	FED(R)	0.124	0.369	0.068	0.318	0.379	0.167	0.146	0.028	0.227	0.024	0.151

* FV is the free-valence index; FED(E), FED(N), and FED(R) are the frontier electron densities for electrophilic, nucleophilic, and radical substitution.

2-Phenylthiazole reacts with electrophiles similarly to the oxazole analog but is much less reactive. This is confirmed upon nitration of an equimolar mixture of PO and PT by N-nitropicolinium tetrafluoroborate in CH_3CN, which excludes protonation [12]. PT is more reactive toward competitive nitration of equimolar mixtures of PO and PT in conc. H_2SO_4, which directs to the benzene ring. It is noteworthy that conditions producing high yields of both 2-(nitrophenyl)thiazoles and 2-(nitrophenyl)oxazoles have been found. It is important that the ratio of isomers formed upon nitration of PO and PT in H_2SO_4 differs greatly. Whereas nitration occurs in the *para* position (ratio of *o*-, *m*-, and *p*-isomers = 3:8:89) for PT, PO is nitrated primarily in the *meta* position [12]. Thus, an oxazole ring protonated on the nitrogen atom is a stronger electron-withdrawing substituent than a protonated thiazole ring.

Table 1 contains the free-valence (FV) indices and frontier electron density (FED) for azocycles that correspond to the three types of reactions: electrophilic [FED(E)], nucleophilic [FED(N)], and radical substitution [FED(R)]. The values were calculated by the PPP/S-CI method. The data show a certain amount of similarity for carbon atoms playing significantly different roles in these types of reactions. For the oxazole ring, only the carbon atoms can be chemically active: for $C_{(2)}$, $C_{(4)}$, and $C_{(5)}$ the FV indices are 0.482, 0.498, and 0.386, respectively. Atom $C_{(5)}$ has the largest index for electrophilic substitution, FED(E) = 0.851; $C_{(2)}$, for nucleophilic substitution, FED(N) = 0.856; and $C_{(2)}$ and $C_{(5)}$, for radical substitution, FED(R) = 0.698 and 0.684, respectively. Atom $C_{(4)}$ plays a small role in electrophilic substitution, FED(E) = 0.077.

For the 2-MeO compound, the methyl group and atom $C_{(5)}$ have the largest FV indices, 1.379 and 0.532, respectively. An estimate of the maximal FED suggessts that the 5- and 2-positions are highly reactive: for $C_{(5)}$ and $C_{(2)}$, FED(E) = 0.853 and 0.853; FED(N) = 0.397 and 0.777, FED(R) = 0.712 and 0.587, respectively.

For PO and PT, C atoms of the benzene and heterocyclic rings have greatly differing indices (Table 1). For electrophilic substitution of PO, $C_{(5)}$ has the largest indices: FV = 0.507 and FED(E) = 0.581. Atoms $C_{(2)}$ and $C_{(4)}$ are possible to compete with it: FV = 0.243, FED(E) = 0.310 and FV = 0.385, FED(E) = 0.277, respectively. Atoms $C_{(2')}$, $C_{(3')}$, $C_{(4')}$, and $C_{(5')}$ also can compete (FV = 0.396-0.423). In nucleophilic and radical substitution reactions, competition can arise among the atoms of the benzene ring: for $C_{(1')}$ and $C_{(4')}$, FED(N) = 0.379 and 0.403, respectively; for $C_{(5)}$, $C_{(1')}$, and $C_{(4')}$, FED(R) = 0.372, 0.272, and 0.304, respectively. The largest indices for the protonated species PO–HAn are seen for $C_{(4)}$ and $C_{(5)}$, FV = 0.520 and 0.509, respectively. They are slightly smaller for atoms of the benzene ring: $C_{(2')}$, $C_{(3')}$, $C_{(4')}$, $C_{(5')}$, and $C_{(6')}$ have FV = 0.423, 0.396, 0.407, 0.396, and 0.423, respectively. For electrophilic substitution, $C_{(4)}$ and $C_{(5)}$ have the largest indices: FED(E) = 0.553 and 0.709, respectively. These indices for the remaining atoms are much smaller. For nucleophilic and radical substitution, $C_{(2)}$ has the largest indices: FED(N) = 0.582 and FED(R) = 0.369. However, the other atoms can compete with it. Apparently protonation of the nitrogen atom and deactivation of the heterocycle can change the course of the reactions.

2.2. Comparison of Quantum-Chemical and NMR Data

Electron density and changes in it that are caused by complexation with $AlCl_3$ and protonation are analyzed by comparing ^{13}C NMR spectra with quantum-chemical calculations using PPP/S-CI [9], CNDO/2 [31], and INDO/S-CI [19] methods. We performed a similar comparison in the present work. Parameters of the ^{13}C NMR spectra have been reported [31]. Changes in the ^{13}C chemical shifts δ_i indicate that carbon atoms in the 2- and 5-positions are deshielded upon protonation and complexation with $AlCl_3$ for both PO and PT. On the other hand, the shielding increases for $C_{(4)}$. Furthermore, the chemical shifts of the carbon atoms of the benzene ring change predictably on going from the free bases to the protonated or complexed species. They increase for *o*-C, *m*-C, and *p*-C and decrease for the substituted *ipso*-C.

Calculations [31] show that protonation of the oxygen of the oxazole is energetically unfavorable, although it is sometimes considered possible. Changing from a vacuum to a polarizing dielectric makes it even more energetically unfavorable. A comparison of the ^{13}C δ_i values and the total charges $\rho\pi_z^{oi}$ indicates that the increase of δ_i for $C_{(5)}$ upon protonation and complexation is due to delocalization of positive charge onto the aromatic system of the heterocycle for both PT and PO. Positive charge is observed to be delocalized not only onto the aromatic system of the heterocycle but also onto the atoms of the benzene ring. However, the heterocycle, the

nitrogen atom of which is directly bonded to the Lewis acid, is deactivated more upon complexation than the benzene ring. This changes the course of electrophilic substitution to attack not at the heterocycle but at the benzene ring.

The deshielding and increased positive charge at $C_{(5)}$, which undergoes electrophilic attack in the free base, are consistent with the considered deactivation of the heterocycle and the change in the course of electrophilic substitution. The behavior of the corresponding phenyl- and methylsubstituted azoles is completely analogous and the chemical shifts in identical positions of the heterocycle are quite similar [31].

Values of σ_p^+ for unprotonated and protonated oxazol-2-yl and thiazol-2-yl as substituents were calculated [31] by using the linear correlation between the changes of the *p*-C chemical shifts relative to unsubstituted benzene $\Delta\delta p$ and the electrophilic substituent constants σ_p^+. Whereas the unprotonated residues have little effect on the reactivity and are practically identical ($\sigma_p^+ = +0.3$), protonation significantly deactivates the benzene ring, much more so for PO ($\sigma_p^+ = 1.1$) than for PT ($\sigma_p^+ = 1.0$). This is also consistent with the reported competitive nitration of PO and PT in conc. H_2SO_4.

2.3. Structural Dependence of Spectral and Fluorescence Properties of Azoles

X-ray structural data indicate that nonfused systems consisting of directly bonded aromatic and(or) heteroaromatic rings are planar in the crystalline state (the molecular symmetry is no greater than C_s). However, the ground state in the gas phase or solution can include conformers with an angle of 35-45° between the rings [32]. The molecular absorption is consistent with that of an array of all conformers under conditions where UV spectra are recorded [39].

The absorption coefficient for monocycles in solution is $\varepsilon_{abs}^{max} = (5\text{-}8)\cdot10^{3}$ $M^{-1}\cdot cm^{-1}$. However, even for the bicyclic molecules PO and TO the UV spectra of solutions and vapors exhibit an intense and broad long-wavelength absorption band (LAB) with $\varepsilon_{abs}^{max} = (25\text{-}43)\cdot10^{3}$ $M^{-1}\cdot cm^{-1}$. Therefore, the absorption cross section sharply increases (up to $\sigma_{13}^{max} \approx 10^{-16}$ cm^2) at the LAB maximum (Table 2). Bathochromic shifts of the LAB and fluorescence bands are observed if the oxygen atom is replaced by sulfur atom (going from PO to PT). The Stokes shift $\Delta\lambda_{ST}$ increases from 45 and 46 to 64 and 68, respectively. The frequency of the 0-0 transition decreases by 2000 cm^{-1} (Table 2).

The parameters ε_{abs}^{max} and σ_{13}^{max} change by several orders of magnitude as the number of subsystems of a single or multiple types increases, i.e., on going from mono- to bicyclic compounds. However, the fluorescence quantum yield, although it remains small, increases by more than two orders of magnitude, from $\gamma \approx 0.0001$ to 0.01-0.04. Clearly both changing the nature of the heterocycle and increasing the number of rings to two increases the rate constant of intercombinational conversion k_{ST} from $\sim10^{10}$ to $\sim0.5\cdot10^{9}$ sec^{-1}. Also, the rate constant of radiative decay k_{fl} decreases from $\sim10^{6}$ (monocycles) to $\sim10^{8}$ sec^{-1} (bicycles). The oscillator cross section (σ_{31}^{osc}) is $<0.3\cdot10^{-18}$ cm^2 (Table 2).

A noticeable bathochromic shift of LAB by λ_{abs}^{max} = 1-3 nm and of the fluorescence band by $\lambda_{osc,fl}^{abs}$ = 2-10 nm is observed for an insignificant change of γ, k_{fl}, and k_{ST} in solvents (cyclohexane, toluene, ethanol, DMF, DMSO, diethyleneglycol) ordered according to increasing dielectric constant and viscosity or ability to associate. The quantity $\sigma_{31}^{osc,max}$ also changes little in different solvents. The bicyclic molecules did not emit light in the solutions. Only weak fluorescence (slightly more intense for the S-containing compounds) was observed even though the power density of the UV laser pumping pulse (without attenuation of the photon flux) was >35 mW/cm^2 [15, 18]. Thus, the irradiated molecules effectively convert the pumping energy into only thermal energy and their triplet states are populated owing to the high rates of intercombinational conversion.

The extinction coefficients, as before, remain high under conditions where PO and PT are protonated, $\varepsilon_{abs}^{max} = (34\text{-}43)\cdot10^{3}$ $M^{-1}\cdot cm^{-1}$. However, a significant bathochromic shift of LAB in the UV spectra and the fluorescence band is observed. The bathochromic shifts of LAB are 8 and 28 nm; of $\lambda_{osc,fl}^{max}$, 22 and 14 nm, if the stable species PO–HAn and PT–HAn,* respectively, are formed in an ethanol–H_2SO_4 mixture. For PO–HAn, the

* These species were formed by increasing the H_2SO_4 content until the spectral and luminescence characteristics did not change. The nature of the complex formed (H-bonded complex or ion pair) requires further study.

TABLE 2. Optical Properties of Molecules in Solutions (Experimental Values) and in the Free State (INDO/S and PPP/S Calculations)

Compound	Solvent (calculation method)	ν_{abs}^{max}, cm^{-1}	λ_{abs}^{max}, nm	ν_{fl}^{max}, cm^{-1}	λ_{fl}^{max}, nm	ν_{00}, cm^{-1}	ν_{00}, nm	γ	$\varepsilon_{abs}^{max} \cdot 10^{3}$, $M^{-1} \cdot cm^{-1}$	$k_{fl} \cdot 10^{9}$, sec^{-1}	$k_{ST} \cdot 10^{9}$, sec^{-1}	$\sigma_{13}^{max} \cdot 10^{16}$, cm^2	$\sigma_{31}^{osc} \cdot 10^{16}$, cm^2
Benzene	Heptane	55556 50000 43478- 38462	180; 200 230-260	—	—	—	—	0.0001	0.002	~0.001	-0.1	<<0.0001	~0.0001
2-Methyl-oxazole	Cyclohexane	48076	208	—	—	—	—	0.0001	0.007	~0.001	-0.1	<<0.0001	~0.0001
2-Phenyl-oxazole (PO)	Cyclohexane	38022	263; 264	32467	308; 310	35250	284; 285	0.01; 0.01	23.6; 42.1	0.005	0.50; 0.52	0.9; 1.6	0.0028
	Ethanol	37878	272	32258	336	35070	301	0.01	43.2	0.005	0.40	16.6	0.0013
	Ethanol–H_2SO_4	36764		29761		32895				0.004			0.0015
	(INDO/S-CI)	36900	271; 239	35971	278; 283	34100	293; 263	0.001	25.0; 25.0	0.001	0.56; 0.68	9.60; 9.8	0.0007
	(PPP/S-CI)	41841		35335		38080		0.001		0.001			0.0005
2-Phenyl-thiazole (PT)	Cyclohexane	36764	272; 274	29761	336; 342	33260	315; 304	0.01; 0.03	27.2; 31.3	0.005	0.13; 0.10	1.05; 1.21	0.002
	Ethanol	36496	296	29239	356	32900	326	0.01	34.1	0.001	0.12	1.31	0.001
	Ethanol–H_2SO_4	33783		28409		30937				0.002			0.001
	(INDO/S-CI)	36363	275; 270	29411	340; 334	32895	304; 299	0.003	25.0; 25.0	0.001	0.15; 0.58	0.96; 0.96	0.0007
	(PPP/S-CI)	37037		29940		33410		0.002		0.001			0.0008

* The following molecular properties are given:
λ_{abs}^{max} (ν_{abs}^{max}), λ_{fl}^{max} (ν_{fl}^{max}), λ_{00} (ν_{00}) – wavelengths and frequencies of UV absorption, fluorescence, and electronic 0-0 transition maxima;
ε_{abs}^{max} – extinction coefficient at long-wavelength UV absorption maxima;
γ – fluorescence quantum yield;
k_{fl}, K_{ST} – rate constants of radiative decay and intercombinational conversion;
σ_{13}^{max} and σ_{31}^{osc} (σ_{31}^{fl}) – absorption and stimulated-emission cross sections.

shift of $\lambda_{osc,fl}^{max}$ is 3.5 times greater than that of λ_{abs}^{max}. However, the analogous shift for PT–HAn is 1.57 times less. The bathochromic shift of $\lambda_{osc,fl}^{max}$ for PO–HAn is two times greater than for PT–HAn (compared with ethanol solutions). According to the literature [18], λ_{abs}^{max} and $\lambda_{osc,fl}^{max}$ exhibit such behavior owing to a change in the way the electronic excitation is localized on the active groups responsible for the most intense vibrational manifolds in the optical spectra of PO and PT in various aggregate states. Therefore, the electron-density distribution among the atoms and bonds in the excited states that affects the characteristics of their transitions caused by external perturbations must be analyzed in detail.

2.4. Excited State Structure and Transition Characteristics

Figures 1-4 show the energy levels of the excited electronic singlet (S_i*) and triplet (T_j) states of benzene (P), oxazole (O), PO, and PT. The literature data [17] clearly show that transitions for benzene (all states of the $\pi\pi$*-type) from lower states $S_{1,2}$* are symmetry forbidden (benzene symmetry is D_{6h}) whereas transitions from high-lying states $S_{3,4}$* with oscillator strength $f_e^{osc} = 1.198$ are allowed (Fig. 1). The transitions $S_{1/2}^* \rightarrow S^0$ occur from MO ψ_2 into ψ_4 and from ψ_2 into ψ_5. Deconvolutions of the MOs into AOs with coefficients of at least 0.097 in absolute value are listed below.

$$\psi_2 = \psi_{HZ} = 0.279\varphi_2 + 0.298\varphi_5 + 0.577\varphi_6,$$
$$\psi_4 = \psi_{VIRT} = 0.369\varphi_1 + 0.200\varphi_3 + 0.369\varphi_5 + 0.200\varphi_6,$$
$$\psi_5 = \psi_{VIRT} = 0.444\varphi_1 + 0.097\varphi_2 + 0.097\varphi_4 + 0.044\varphi_5.$$

MOs ψ_3 and ψ_4 are involved in the electronic transition $S_3^* \rightarrow S_0$. The transition has the magnitude $|\psi_{HZ \rightarrow VIRT} = \psi_{3 \rightarrow 4}|^2 = 0.5$, whereas the $S_4^* \rightarrow S_0$ transition is $|\psi_{HZ \rightarrow VIRT} = (\psi_{2 \rightarrow 4} + \psi_{2 \rightarrow 5})|^2 = (0.5 + 0.5) = 1$.

The triplet transition $T_1 \rightarrow S_0$ is described by the contributors $2 \rightarrow 5$ ($|\psi_{HZ \rightarrow VIRT}|^2 = 0.446$), $3 \rightarrow 4$ ($|\psi_{HZ \rightarrow VIRT}|^2 = 0.446$), and $3 \rightarrow 5$ ($|\psi_{HZ \rightarrow VIRT}|^2 = 0.108$). Thus, alternation is typical of MOs for free benzene.

Figure 2 shows that the fluorescence transition $S_1^* \rightarrow S_0$ in oxazole is symmetry allowed with $f_e^{osc} = 0.283$, $\nu_{0-0}^{osc} = 49{,}720\ cm^{-1}$, and $|\psi_{HZ \rightarrow VIRT}|^2 = 0.835$. The MOs 3 and 4 deconvolute into AOs as follows:

$$\psi_3 = \psi_{HZ} = 0.519\varphi_1 + 0.196\varphi_4 + 0.088\varphi_5,\ \psi_4 = \psi_{VIRT} = 0.654\varphi_1 + 0.509\varphi_2.$$

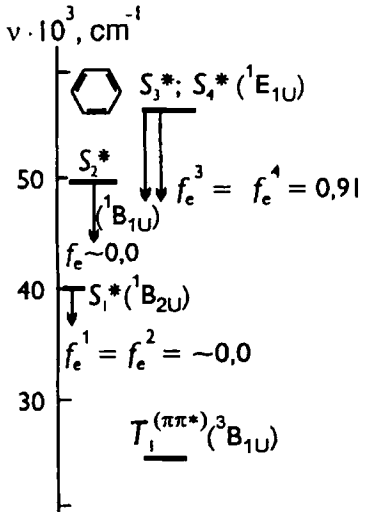

Fig. 1. Diagram of excited singlet (S_i*) and triplet (T_i) states and transitions in benzene. Arrows indicate the oscillator strengths of $S_i^* \rightarrow S_0$ transitions.

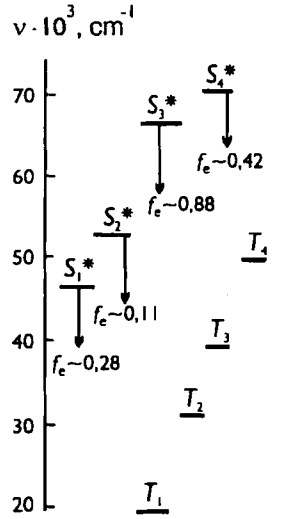

Fig. 2. Diagram of excited singlet (S_i*) and triplet (T_i) states and transitions in oxazole. Arrows indicate the oscillator strengths of $S_i^* \rightarrow S_0$ transitions.

TABLE 3. Energetics (eV) of Molecules from PPP Data

Compound	Electronic energy	π-Binding energy	σ-Binding energy	Total binding energy	Atomization energy	Solvation factor in ground state
Benzene	-77,03	-10,07	-22,03	-32,09	-32,10	
Oxazole	-100,80	-8,95	-17,63	-26,57	-26,57	
2-Methyloxazole	-150,48	-10,6	-17,69	-28,29	-28,29	1,379
2-Phenyloxazole	-178,41	-19,57	-43,64	-63,21	-63,21	1,159
2-Phenylthiazole	-165,25	-16,83	-42,13	-58,97	-58,97	0,256
PO–HAn complex	-190,5	-23,79	-43,78	-67,58	-67,58	3,610

The quantities $f_e^{osc} = 0.436$ (twice as large) and $\nu_{0-0}^{osc} = 49{,}768$ cm^{-1} (small increase) for the $S_1^* \rightarrow S_0$ fluorescence transition of the 2-MeO molecule are caused by the presence of the methyl group. The one-electron transition coefficient $|\psi_{HZ} \rightarrow \psi_{VIRT}|^2 = 0.918$. In this instance, the MOs 4 and 5 deconvolute into AOs as follows:

$$\psi_4 = \psi_{HZ} = 0.443\varphi_4 + 0.653\varphi_5 + 0.221\varphi_6,\ \psi_5 = \psi_{VIRT} = 0.623\varphi_2 + 0.534\varphi_5.$$

Calculations indicate that the σπ-electron energy (total bonding energy) regularly increases in the order benzene–oxazole–2-methyloxazole: $E_{\sigma\pi}^{bond} \approx$ -77.03, -100.82, and -150.48 eV. The ratio of the σ- and π-contributions are approximately 2.2, 1.98, and 1.7 eV, respectively (Table 3). The solvation multiplier increases: $M_0^{solv} = 1.19$ and ~1.38 eV (for the O and 2-MeO molecules, respectively).

The total bonding energies on going to the bicyclic molecules PO and PT are $E_{\sigma\pi}^{bond} =$ -63.21 and -58.97 eV; the ratio $E_\sigma^{bond}/E_\pi^{bond} \approx$ -2.23 and 2.5, respectively. Thus, the contribution of the σ-component to the total energy of the molecule and its bonds in all instances predominates.

The parameters $\nu_{0-0}^{osc} = 38{,}080$ cm^{-1} and $f_e^{osc} = 0.8$ (PPP/S-CI method) and $\nu_{0-0}^{osc} = 34{,}100$ cm^{-1} and $f_e^{osc} = 0.63$ (INDO/S-CI method) are obtained for the fluorescence transition of PO (for PO–HAn,* $\nu_{0-0}^{osc} = 33{,}160$ cm^{-1} and $f_e^{osc} = 0.76$). For PT, $\nu_{0-0}^{osc} = 33{,}410$ cm^{-1} and $f_e^{osc} = 0.71$ (PPP/S-CI method). Thus, replacement of oxygen atom by sulfur atom changes the energy of the polyatomic system and causes a large bathochromic shift of the frequency of the 0–0 electronic transition by $\nu_{0-0}^{osc} = 4{,}700$ cm^{-1}. Protonation produces a shift $\nu_{0-0}^{osc} = 4{,}670$ cm^{-1} [33]. The fluorescence transitions are monoconfigurational and the MOs are deconvoluted into AOs as follows for PO:

$$\psi_6 = \psi_{HZ} = 0.372\varphi_4 + 0.539\varphi_5 + 0.288\varphi_6 + 0.258\varphi_7 + 0.242\varphi_{11},$$
$$\psi_7 = \psi_{VIRT} = 0.331\varphi_2 + 0.014\varphi_4 + 0.285\varphi_6 + 0.534\varphi_7 + 0.449\varphi_9,$$

for PO–HAn:

$$\psi_6 = \psi_{HZ} = 0.526\varphi_4 + 0.596\varphi_5 + 0.261\varphi_6 + 0.217\varphi_7 + 0.185\varphi_{11},$$
$$\psi_7 = \psi_{VIRT} = 0.539\varphi_2 + 0.205\varphi_4 + 0.261\varphi_6 + 0.217\varphi_7 + 0.394\varphi_9,$$

for PT:

$$\psi_6 = \psi_{HZ} = 0.149\varphi_1 + 0.390\varphi_3 + 0.132\varphi_4 + 0.292\varphi_7 + 0.128\varphi_8 + 0.108\varphi_{10} + 0.149\varphi_{11},$$
$$\psi_7 = \psi_{VIRT} = 0.387\varphi_4 + 0.559\varphi_5 + 0.271\varphi_6 + 0.235\varphi_7 + 0.230\varphi_{11}.$$

Thus, the carbon atom in the 5-position of the oxazole ring makes the main contribution to the HOMO for bicyclic molecules upon deconvolution of the MOs into AOs. Atoms $C_{(2)}$ and $C_{(4)}$ and the carbon atom in the *p*-position of the benzene ring contribute most to the LUMO.

* Protonation was effected in the PPP method by choosing parameters that represent the change of coordination of the nitrogen atom such that the calculated photophysical characteristics agreed with the experimental spectrum of PO in ethanol with added conc. H_2SO_4 (see above).

2.5. Comparative Evaluation of the Reactivity and Properties of the Excited States and Transitions

2.5.1. Fluorescence Characteristics. According to the literature [18], the different shifts of λ_{abs}^{max}, $\lambda_{0\text{-}0}$, and λ_{osc}^{max} in optical spectra are consistent with a change in the nature of the vibronic interactions of the bonds in the lower excited states of PO and PT. This in turn should affect the electron-density distribution in the ground state.

Figures 3 and 4 show that electronic transitions $S_0 \rightarrow S_{1\text{-}6}$ with different intensities and polarizations appear in the UV absorption spectra of PO and PT. Differences in the localization of the excitation that are evident in the charges (Σqi), localization indices (ΣL_i), and bond orders ($\Delta p_{\mu\nu}$) of atoms, bonds, and rings in the electronic excited states S_i* and T_j determine the differences in the oscillator strength (f_{fl}) and frequencies (ν_i*) of the $S_0 \rightarrow S_{1\text{-}6}$ transitions. The properties of highly excited states will not be discussed in the present work. However, the basic trends in the change of the noted parameters are clearly seen by analyzing the data in Tables 4-6.

The difference in the frequencies ν_{abs}^{max}, $\nu_{0\text{-}0}$, and ν_{fl}^{max} for cyclohexane solutions of PO and PT are 1258, 1010, and 3706 cm^{-1}, respectively. It is important that the largest changes in the ^{13}C NMR chemical shifts on replacement of oxygen atom by sulfur atom (on going from PO to PT) occur for the azocycles [31]. The data in Table 2 and Figs. 1-4 indicate that the difference between the frequencies of the 0–0 electronic transition for a cyclohexane solution of PO (closest to the optical properties of organic molecules in dense vapors [18]) that are calculated from the UV absorption and fluorescence spectra and by the INDO/S-CI and PPP/S-CI methods are: $\Delta\nu_{0\text{-}0} = \nu_{0\text{-}0}^{exp} - \nu_{0\text{-}0}^{theor}$ = 35,250 - 34,100 = 1150 cm^{-1} (INDO/S-CI) and 38,100 - 34,100 = 4,000 cm^{-1} (PPP/S-CI). However, this difference is less for PT: 33,260 - 32,895 = 465 cm^{-1} (INDO/S-CI) and 33,260 - 33,410 = -150 cm^{-1} (PPP/S-CI). Thus, the energy of polyatomic molecules in the free state and solution is different. The differences in the solvation coefficients of the electronic systems in PO and PT are responsible for this (see Sects. 2.4 and 2.6).

A strong bathochromic shift is seen for the 0–0 transition upon complexation and protonation in ethanol solution: for PO and PO–HAn the frequency difference is $\Delta\nu_{0\text{-}0}$ = 35,070 - 32,895 = 2,175 cm^{-1}; for PT and PT–HAn, 32,900 - 30,937 = 1,963 cm^{-1}. Hence, the change in the nature of the vibronic interactions in PT–HAn compared with PO–HAn upon complexation and protonation of the nitrogen atom and formation of a stable adduct is related primarily to the change in the electron-density distribution on the heterocycle.

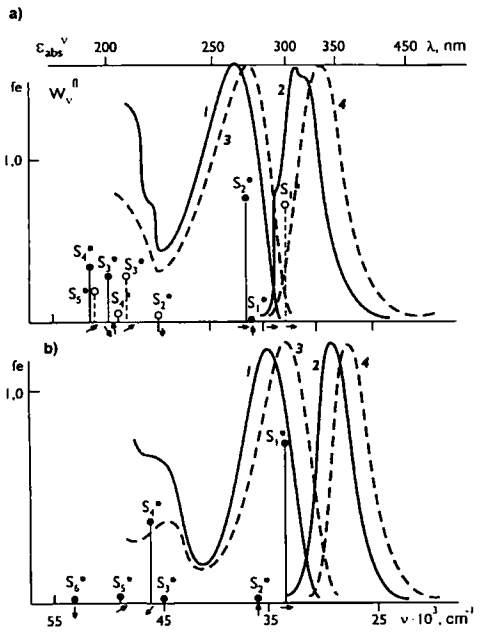

Fig. 3. UV absorption ε_{abs}^{ν} (1, 3) and fluorescence ω_{ν}^{fl} (2, 4) spectra of 2-phenyloxazole (a) and 2-phenylthiazole (b) in ethanol (1, 2) and ethanol–H_2SO_4 (3, 4). Vertical lines denote oscillator strengths (f_e) of $S_0 \rightarrow S_n$* electronic transitions from PPP/S calculations for the free states of PO and PT (solid lines) and the PO–HAn adduct (dashed lines). Arrows under the vertical lines show the polarization of the electronic transitions. An arrow along the abscissa denotes that the electronic transition is polarized along the molecular axis; otherwise, at an angle.

TABLE 4. Charges on Atoms and Heterocycle (Σq), Dipole Moments (d), and Solvation Factors (M*)

Compound	E. s.*[2]	$O_{(1)}$	$C_{(2)}$	$N_{(3)}$	$C_{(4)}$	$C_{(5)}$	$C_{(1')}$	$C_{(2')}$	$C_{(3')}$	$C_{(4')}$	$C_{(5')}$	$C_{(6')}$	Σq	d, D	M_O^{solv}
1	2	3	4	5	6	7	8	9	10	11	12	13	14	15	16
Oxazole	S_0	0.223	-0.254	-0.468	0.314	0.185								2.96	1.191
	S_1*	0.296	0.192	-0.093	-0.219	-0.176								5.32	-2.494
	S_2*	0.330	-0.078	-0.032	0.043	-0.262								3.84	-1.427
	S_3*	0.539	-0.092	-0.050	-0.208	-0.188								1.40	-1.272
	S_4*	0.855	-0.271	-0.375	-0.002	-0.207								3.80	-3.051
	S_5*	0.926	0.128	-0.423	-0.439	-0.192								3.38	-3.870
	T_1	0.193	-0.018	-0.231	-0.081	-0.061								1.79	-0.647
	T_2	0.308	0.068	-0.351	-0.127	0.103								4.23	-1.725
	T_3	0.568	-0.444	-0.286	0.276	-0.114								4.29	-4.490
	T_4	0.541	0.064	0.102	-0.321	-0.386								5.11	-3.880
	T_5	0.536	-0.163	-0.177	0.020	-0.216								3.05	-3.039
	T_6	0.023	0.082	-0.499	-0.440	-0.167								3.38	-3.870
2-Phenyl-oxazole	S_0	0.328	0.031	-0.270	0.002	-0.094	-0.012	-0.017	0.005	0.005	0.000	-0.013	-0.003	2.86	1.159
	S_1*	0.317	0.003	-0.274	0.024	-0.054	-0.019	0.108	-0.043	0.000	0.032	-0.123	0.045	2.07	-1.455
	S_2*	0.274	0.030	-0.325	0.126	0.099	-0.083	-0.114	0.032	-0.048	-0.043	0.052	0.203	5.80	-1.552
	S_3*	0.287	-0.008	-0.287	0.120	-0.043	0.003	0.019	-0.022	0.013	0.040	-0.120	0.068	2.46	-1.306
	S_4*	0.303	0.097	-0.270	0.087	0.063	-0.049	-0.089	0.002	-0.025	-0.096	-0.023	0.281	6.04	-1.514
	S_5*	0.279	0.000	-0.182	-0.032	-0.119	0.009	0.060	0.002	0.002	-0.035	0.016	-0.054	2.28	-0.973
	S_6*	0.344	-0.011	-0.219	0.019	0.015	-0.070	0.021	-0.019	-0.044	-0.008	-0.028	0.148	3.96	-1.428
	T_1	0.287	0.017	-0.259	0.036	-0.062	-0.017	0.009	0.003	-0.000	0.001	-0.015	0.018	2.49	-1.126
	T_2	0.242	0.034	-0.254	0.058	-0.077	-0.011	0.016	0.005	0.002	0.000	-0.017	0.004	2.03	-0.905
	T_3	0.322	0.030	-0.273	0.008	-0.084	-0.034	0.023	0.022	-0.014	0.007	-0.008	0.004	2.75	-1.383
	T_4	0.324	0.064	-0.286	-0.037	-0.062	-0.015	0.048	-0.019	0.007	0.020	-0.045	0.004	3.07	-1.472
	T_5	0.331	0.028	-0.297	-0.084	0.027	-0.013	0.013	0.006	0.005	0.007	-0.022	0.026	3.64	-1.560
	T_6	0.321	0.032	-0.268	0.014	-0.071	-0.014	-0.005	0.063	0.033	-0.070	-0.032	0.196	2.04	-1.400

TABLE 4 (continued)

1	2	3	4	5	6	7	8	9	10	11	12	13	14	15	16
2-Phenyl-thiazole	S_0	0.066	0.140	-0.229	0.028	-0.037	-0.015	0.023	0.002	0.012	0.000	0.009	-0.032	1.80	0.256
	S_1*	0.090	-0.017	-0.320	0.179	0.124	-0.021	0.002	-0.002	-0.007	0.007	-0.038	0.058	3.35	-0.779
	S_2*	0.063	0.094	-0.251	0.034	-0.043	-0.033	0.028	0.050	-0.021	0.042	0.038	-0.103	2.82	-0.417
	S_3*	0.807	-0.168	-0.268	0.004	-0.238	-0.032	-0.029	0.000	-0.026	0.005	-0.055	0.137	5.06	-3.907
	S_4*	0.119	-0.078	-0.392	0.131	-0.012	0.115	-0.019	0.041	0.089	0.042	-0.038	-0.231	3.96	-1.079
	S_5*	0.064	0.058	-0.239	0.085	0.047	0.025	-0.009	-0.016	0.045	-0.045	-0.015	0.016	1.58	-0.373
	S_6*	0.073	0.124	-0.130	0.021	0.044	-0.095	0.065	-0.039	-0.062	-0.038	0.036	0.133	2.85	-0.280
	T_1	0.039	0.036	-0.217	0.091	0.025	-0.003	0.017	0.002	0.005	0.000	0.004	-0.026	1.09	-0.278
	T_2	0.064	0.143	-0.217	0.019	-0.035	-0.001	0.012	0.004	0.009	0.002	0.001	-0.027	1.74	-0.338
	T_3	0.068	0.100	-0.258	0.011	-0.023	-0.059	0.130	0.033	-0.044	0.078	-0.034	-0.102	2.61	-0.528
	T_4	0.070	0.103	-0.254	0.010	-0.016	-0.039	-0.018	0.062	-0.028	0.017	0.091	-0.087	2.91	-0.460
	T_5	0.120	0.073	-0.274	0.000	0.025	-0.016	0.020	0.012	0.017	0.022	-0.001	-0.056	2.55	-0.479
	T_6	0.097	0.102	-0.221	0.038	-0.021	0.080	-0.078	-0.019	0.177	-0.079	-0.076	0.136	1.70	-0.570
PO–HAn complex	S_0	0.360	0.302	-0.778	0.169	-0.125	-0.036	0.057	0.008	0.029	-0.001	0.008	-0.072	5.37	3.610
	S_1*	0.286	-0.015	-0.826	0.373	0.186	-0.005	0.070	-0.004	0.004	0.020	-0.076	0.004	5.93	-4.970
	S_2*	0.327	0.189	-0.797	0.170	-0.116	-0.058	0.000	-0.105	-0.050	0.078	0.081	-0.226	6.80	-4.622
	S_3*	0.270	0.085	-0.828	0.209	-0.043	0.130	0.020	0.062	0.125	0.058	-0.069	-0.306	7.10	-4.520
	S_4*	0.335	0.130	-0.798	0.274	0.022	0.045	0.096	-0.027	0.116	-0.061	-0.055	-0.038	4.70	-4.670
	S_5*	0.365	0.192	-0.784	0.274	0.020	-0.074	-0.034	-0.010	-0.041	-0.079	0.022	0.067	5.20	-4.840
	S_6*	0.337	0.262	-0.795	0.340	0.110	-0.025	0.070	-0.087	0.052	-0.081	-0.079	0.254	7.90	-5.180
	T_1	0.343	0.167	-0.799	0.252	-0.024	0.011	0.032	0.009	0.013	0.006	-0.011	-0.061	5.02	-4.617
	T_2	0.318	0.071	-0.845	0.297	0.170	-0.036	0.044	0.009	0.004	-0.001	-0.031	0.011	6.00	-5.077
	T_3	0.321	0.416	-0.782	0.056	-0.104	-0.035	0.072	0.008	0.034	-0.001	0.015	-0.094	6.34	-4.836
	T_4	0.323	0.206	-0.798	0.158	-0.132	-0.170	0.152	0.159	-0.133	0.167	0.068	-0.243	7.24	-5.021
	T_5	0.341	0.253	-0.788	0.180	-0.107	0.001	0.054	0.018	0.001	0.037	-0.051	-0.121	5.69	-4.621
	T_6	0.364	0.264	-0.777	0.190	-0.098	0.111	-0.112	0.027	0.341	-0.156	-0.153	-0.058	5.25	-5.495

* The PPP/S method gave the following charges for atoms of 2-methyloxazole in the ground state: $Q_{(1)}$ 0.287, $C_{(2)}$ 0.131, $N_{(3)}$ -0.374, $C_{(4)}$ -0.153, $C_{(5)}$ 0.110.

*[2] Electronic states.

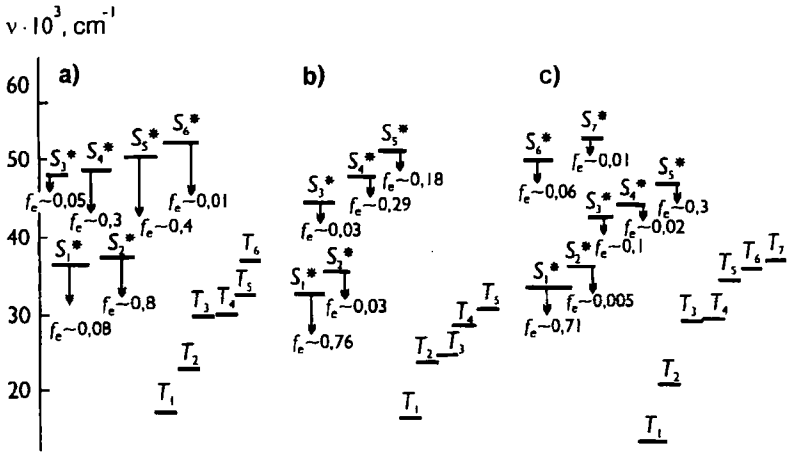

Fig. 4. Diagram of excited singlet (S_i*) and triplet (T_i) states and transitions: 2-phenyloxazole (a), protonated 2-phenyloxazole (b), 2-phenylthiazole (c). Arrows indicate oscillator strengths of $S_i^* \rightarrow S_0$ transitions.

2.5.2. Charge Distribution. A polyatomic irradiated molecule can be represented as a system of excited electronic states S_i* and T_j in which the transformation of excitation-energy quanta is described by electronic, vibronic, and spin–orbit interactions [18-20]. Therefore, we will examine the electronic structure of a wide range of S_i* and T_j states for series of molecules. Tables 4-6 give the calculated properties of the excited singlet and triplet states of oxazole, PO, PT, and PO protonated on the nitrogen atom.

Charges q_e* in the S_1* and T_1 states of oxazole differ not only in magnitude but also in the tendency to change. For example, the largest negative charges in the S_1* state are localized on $N_{(3)}$ and $C_{(2)}$: q_e* = -0.468 and -0.254; for the T_1 state, on $C_{(2)}$, $N_{(3)}$, $C_{(4)}$, and $C_{(5)}$: q_e* = -0.018, -0.231, -0.081, and -0.061, respectively. The charge distribution in the higher lying states S_i* and T_j is much different than in S_1* and T_1 (Table 4). However, an excess of electron density is practically always localized on $N_{(3)}$. Thus, only one site, the nitrogen atom, is possible for attack by an active proton on complexed and protonated oxazole.

The dipole moment of oxazole in the S_1* and T_1 states increases and decreases, respectively (to 5.3 and 1.8 D compared with d_0 = 3 D in the ground state). In the higher lying states S_i* and T_j, it more than doubles. Thus, the contribution of orientation effects (dipole–dipole mechanism) to intermolecular interactions substantially increases upon excitation into any S_i* and T_j. The large increase of M_O^{solv} in triplet states and the small one in singlet states is noteworthy. This indicates that the σπ-electron system of oxazole is more easily solvated upon excitation. Introduction of a methyl group increases d_0 in both the ground (up to d_0 = 4.1 D) and excited electronic states. It also increases the solvation factor M_O^{solv} to 1.38 eV.

A comparison of the charge distribution q_e* and $\sum_i q_i$* on atoms and groups of atoms in PO and PT indicates that replacement of oxygen atom by sulfur atom in the ring decreases the positive charge from 0.274-0.388 ($O_{(1)}$) to 0.063-0.110 ($S_{(1)}$), with the exception of the two states S_3* and S_{10}*, where q_e* on $S_{(1)}$ is 0.807 and 0.337. The largest negative charge, (-0.130 to -0.380) is localized on the nitrogen atom in any of the S_i* and T_j states. However, the $C_{(2)}$ atom bonded to it is more often positively charged: 0.031-0.097 (PO) and 0.036-0.143 (PT), i.e., q_e* is larger for PT. Negative charge is also localized on $C_{(5)}$ of the oxazole or thiazole ring, q_e* = -(0.070-0.012). However, the changes in q_e* alternate depending on the number of the S_i* and T_j excited state. The changes in q_e* in the S_i* and T_j states of the benzene rings are much (by several orders of magnitude) smaller than in the heterocycles (Table 4). For PO, only the amount of charge transfer onto the benzene ring (an electron-density acceptor) changes on going to an electronic state of different multiplicity.

Excitation of PT causes charge to transfer from the benzene onto the heterocycle, or vice versa, depending on the spin of the excited state. For example, the thiazole ring is an electron donor in the S_1* state ($\sum_i q_i$* = 0.058) and an acceptor in the S_0* ($\sum_i q_i$* = -0.032) and T_1 ($\sum_i q_i$* = -0.026) states, i.e., the quantity $\sum_i q_i$* is much less and the $S_1^* \rightarrow S_0$ fluorescence transition is more delocalized in the T_1 state than the $T_1 \rightarrow S_0$ phosphorescence transition.

TABLE 5. Excited Electron Distribution Calculated by the PPP/S Method on Atoms and Heterocycle ($\Sigma L_{\mu i}$, %)

Compound	State*[2]	$O_{(1)}$	$C_{(2)}$	$N_{(3)}$	$C_{(4)}$	$C_{(5)}$	$C_{(1')}$	$C_{(2')}$	$C_{(3')}$	$C_{(4')}$	$C_{(5')}$	$C_{(6')}$	$\Sigma L\mu i$
1	2	3	4	5	6	7	8	9	10	11	12	13	14
Oxazole	S_1*	8.2	34.8	12.0	17.6	27.3							
	S_2*	6.6	20.3	17.6	23.7	31.8							
	S_3*	10.3	16.6	22.7	27.5	22.9							
	S_4*	10.8	13.0	42.4	28.1	5.7							
	S_9*	42.2	30.3	8.8	1.8	16.8							
	S_{10}*	30.2	10.9	14.7	26.2	36.7							
	T_1	7.7	27.9	7.8	19.9	36.7							
	T_2	2.3	26.6	24.2	24.7	22.3							
	T_3	23.0	24.7	26.2	18.9	7.2							
	T_4	15.3	6.6	30.3	27.9	19.9							
	T_9	25.3	27.3	15.1	10.2	22.1							
	T_{10}	34.7	12.9	14.7	23.3	14.4							
2-Phenyl-oxazole	S_1*	1.1	2.5	3.3	1.2	4.0	12.7	16.0	14.6	13.8	14.0	16.7	12.2
	S_2*	3.8	14.2	9.5	6.5	16.9	12.9	9.8	2.2	12.3	2.7	9.1	50.9
	S_3*	3.3	9.5	8.7	9.4	10.9	11.1	13.6	4.7	10.5	11.5	6.8	41.8
	S_4*	1.5	8.7	5.3	5.6	11.8	6.2	10.7	16.1	6.8	8.4	18.7	33.1
	S_5*	3.3	9.8	6.2	6.9	13.6	4.9	13.3	11.7	5.3	12.4	12.6	39.8
	S_6*	5.6	18.1	16.8	11.0	14.8	9.9	4.3	3.1	9.4	2.5	4.5	66.2
	T_1	2.8	7.5	5.4	3.3	10.3	13.3	12.4	9.3	14.0	9.2	12.5	29.3
	T_2	5.5	16.1	3.5	14.1	26.3	2.5	6.7	7.0	4.5	6.9	6.8	65.6
	T_3	0.8	1.0	2.5	0.5	2.1	14.9	18.2	14.7	12.5	14.0	18.2	6.9
	T_4	1.2	3.5	5.2	9.5	8.7	8.8	14.0	12.7	9.7	12.8	13.8	6.8
	T_5	3.6	17.0	18.3	14.9	14.8	4.7	3.8	4.9	9.3	5.0	3.9	28.1
	T_6	0.9	1.5	2.8	0.7	2.7	12.5	17.0	15.3	14.3	15.5	16.9	68.5

TABLE 5 (continued)

1	2	3	4	5	6	7	8	9	10	11	12	13	14
2-Phenyl-thiazole	S_1*	3.6	20.6	13.9	8.8	22.1	7.1	7.1	0.7	8.4	0.8	7.0	69.0
	S_2*	0.5	3.1	5.0	0.3	3.2	10.4	17.1	15.1	13.3	15.0	17.0	12.1
	S_3*	39.9	16.1	14.0	4.2	11.8	2.5	3.7	0.2	3.6	0.5	3.5	86.0
	S_4*	4.9	16.4	9.9	7.3	14.2	14.1	6.7	3.6	12.5	3.4	6.9	52.8
	S_5*	1.1	11.0	8.1	3.9	11.6	3.5	15.7	12.9	4.1	12.6	15.7	35.6
	S_6*	1.0	9.3	5.2	7.8	14.1	12.5	9.6	9.4	12.2	9.1	9.8	37.5
	T_1	1.5	20.5	9.5	17.8	35.0	2.5	4.2	0.7	3.4	0.7	4.1	84.4
	T_2	0.4	2.6	3.7	7.8	9.3	12.2	12.0	12.4	15.7	12.0	12.0	23.8
	T_3	0.7	4.8	7.2	4.4	5.7	8.4	14.2	17.4	8.3	10.0	19.0	22.7
	T_4	0.7	4.9	7.3	4.8	6.1	7.8	19.1	10.1	8.0	17.5	13.8	23.7
	T_5	3.3	11.6	11.5	8.0	9.3	8.7	6.1	9.0	16.8	9.2	6.4	43.7
	T_6	2.0	2.7	4.6	0.8	3.5	10.8	16.1	14.9	13.3	15.0	16.3	13.6
PO-HAn complex	S_1*	7.0	22.7	4.2	25.7	18.0	7.4	7.6	0.8	8.3	1.2	7.4	67.5
	S_2*	2.6	5.8	1.4	1.9	1.9	10.0	17.1	14.9	12.8	14.1	17.6	13.6
	S_3*	4.7	20.0	2.9	5.9	6.8	16.4	8.3	5.5	15.6	5.2	8.7	40.3
	S_4*	3.7	11.1	2.0	7.4	8.5	4.5	14.6	14.0	5.2	12.9	16.1	32.7
	S_5*	2.0	8.2	1.1	6.6	7.4	10.9	15.2	12.0	9.7	15.1	11.6	25.4
	S_6*	1.6	0.9	9.6	12.8	12.2	2.9	11.8	15.4	4.8	14.9	13.1	37.1
	T_1	4.2	8.7	1.8	6.1	8.7	13.4	12.7	9.4	14.9	9.1	13.0	27.5
	T_2	4.3	22.5	3.5	17.9	14.8	1.9	7.4	7.6	4.8	6.9	8.4	63.0
	T_3	4.2	8.0	1.0	5.6	39.6	0.2	1.0	0.5	0.6	0.4	1.1	96.2
	T_4	2.3	4.9	1.3	1.3	1.2	12.4	20.4	13.3	10.4	13.8	18.7	11.0
	T_5	1.6	4.6	0.9	1.5	1.8	11.7	15.4	15.6	15.5	16.0	15.4	10.4
	T_6	1.5	1.9	0.7	1.6	1.9	9.7	15.4	16.4	16.9	19.5	14.9	7.4

TABLE 6. Bond Lengths $l(a - b)$ and Orders $P_{\mu\nu}$

Compound	State	$O_{(1)}$–$C_{(2)}$ or $S_{(1)}$–$C_{(2)}$	$C_{(2)}$–$N_{(3)}$	$N_{(3)}$–$C_{(4)}$	$C_{(4)}$–$C_{(5)}$	$C_{(5)}$–$O_{(1)}$ or $C_{(5)}$–$S_{(1)}$	$C_{(5)}$–$C_{(1')}$	$C_{(1')}$–$C_{(2')}$	$C_{(2')}$–$C_{(3')}$	$C_{(3')}$–$C_{(4')}$	$C_{(4')}$–$C_{(5')}$	$C_{(5')}$–$C_{(6')}$	$C_{(1')}$–$C_{(6')}$
1	2	3	4	5	6	7	8	9	10	11	12	13	14
Oxazole	$l(a\text{-}b)$[a]	1.311	1.316	1.348	1.375	1.321							
	S_0	0.509	0.741	0.560	0.768	0.448							
	S_1*	0.197	0.382	0.563	0.414	0.397							
	S_2*	0.452	0.453	0.477	0.301	0.279							
	S_3*	0.394	0.513	0.248	0.371	0.346							
	S_4*	0.599	0.311	0.088	0.608	0.433							
	S_9*	0.270	0.495	0.583	0.677	0.019							
	S_{10}*	0.223	0.519	0.178	0.379	0.133							
	T_1	0.270	0.495	0.657	0.267	0.275							
	T_2	0.428	0.290	0.330	0.401	0.447							
	T_3	0.230	0.425	0.189	0.673	0.446							
	T_4	0.600	0.508	0.122	0.431	0.220							
	T_9	0.060	0.370	0.464	0.516	0.017							
	T_{10}	0.194	0.506	0.198	0.463	0.165							
2-Methyl-oxazole	$l(a\text{-}b)$	1.314	1.325	1.354	1.371	1.331	1.500						
	S_0	0.488	0.691	0.526	0.811	0.389	0.353						
2-Phenyl-oxazole	$l(a\text{-}b)$[b]	1.360	1.294	1.384	1.347	1.378	1.454	1.385	1.383	1.385	1.385	1.384	1.385
	$l(f\text{-}b)$[c]	1.360	1.294	1.384	1.347	1.378	1.459	1.396	1.383	1.385	1.385	1.384	1.391
	$l(a\text{-}b)$	1.314	1.323	1.346	1.377	1.321	1.461	1.401	1.395	1.397	1.397	1.395	1.402
	$P(S_0)$[d]	1.011	1.295	1.073	1.325	1.034	1.315	1.110	0.730	1.096	0.662	0.674	0.635
	$P(S_1$*)	-0.197	-0.354	0.146	-0.251	0.036	0.235	-0.134	0.043	-0.051	0.948	1.205	1.178

TABLE 6 (continued)

1	2	3	4	5	6	7	8	9	10	11	12	13	14
	S_0*	0.489	0.705	0.570	0.777	0.449	0.295	0.636	0.673	0.663	-0.551	0.043	0.043
	S_1*	0.457	0.649	0.588	0.745	0.449	0.397	0.485	0.516	0.534	0.546	0.515	0.470
	S_2*	0.354	0.477	0.641	0.607	0.433	0.553	0.421	0.720	0.585	0.572	0.721	0.436
	S_3*	0.395	0.602	0.492	0.623	0.439	0.355	0.442	0.609	0.637	0.499	0.608	0.567
	S_4*	0.434	0.583	0.611	0.635	0.367	0.390	0.619	0.487	0.529	0.687	0.485	0.473
	S_5*	0.406	0.593	0.599	0.601	0.410	0.313	0.573	0.476	0.619	0.602	0.479	0.585
	S_6*	0.437	0.382	0.485	0.597	0.407	0.280	0.533	0.697	0.565	0.573	0.702	0.521
	T_1	0.414	0.590	0.616	0.676	0.405	0.423	0.457	0.607	0.503	0.534	0.608	0.455
	T_2	0.345	0.582	0.644	0.404	0.326	0.283	0.614	0.571	0.612	0.613	0.572	0.611
	T_3	0.471	0.674	0.577	0.767	0.447	0.371	0.450	0.494	0.558	0.558	0.495	0.451
	T_4	0.462	0.655	0.506	0.615	0.449	0.352	0.529	0.508	0.576	0.572	0.509	0.532
	T_5	0.455	0.390	0.417	0.560	0.411	0.298	0.595	0.659	0.560	0.559	0.659	0.593
	T_6	0.467	0.664	0.582	0.760	0.448	0.379	0.483	0.497	0.533	0.529	0.499	0.485
2-Phenyl-thiazole	$l(a\text{-}b)$[b]	1.769	1.261	1.19	1.769	1.261	1.513	1.382	1.407	1.385	1.373	1.421	1.378
	$l(f\text{-}b)$[c]	1.77	1.27	1.480	1.54	1.79	—	—	—	—	—	—	—
	$l(a\text{-}b)$	1.750	1.301	1.373	1.356	1.757	1.455	1.402	1.395	1.397	1.394	1.394	1.403
	S_0	0.228	0.825	0.421	0.895	0.199	0.329	0.629	0.673	0.663	0.660	0.677	0.627
	S_1*	0.068	0.488	0.589	0.631	0.259	0.561	0.489	0.717	0.615	0.612	0.718	0.489
	S_2*	0.204	0.749	0.443	0.877	0.193	0.434	0.490	0.492	0.544	0.544	0.495	0.493
	S_3*	0.172	0.582	0.447	0.798	0.043	0.435	0.571	0.689	0.646	0.640	0.688	0.575
	S_4*	0.201	0.606	0.437	0.714	0.048	0.366	0.469	0.717	0.551	0.553	0.718	0.462
	S_5*	0.166	0.639	0.518	0.765	0.199	0.436	0.562	0.445	0.635	0.639	0.459	0.563
	S_6*	0.170	0.716	0.522	0.688	0.216	0.283	0.508	0.605	0.539	0.541	0.609	0.504
	T_1	0.128	0.559	0.632	0.402	0.128	0.429	0.575	0.676	0.646	0.643	0.680	0.573
	T_2	0.210	0.795	0.406	0.735	0.188	0.355	0.496	0.575	0.500	0.505	0.581	0.493
	T_3	0.211	0.718	0.397	0.815	0.191	0.420	0.564	0.458	0.527	0.664	0.485	0.458
	T_4	0.213	0.718	0.396	0.807	0.192	0.413	0.463	0.476	0.668	0.526	0.457	0.578
	T_5	0.243	0.613	0.371	0.752	0.171	0.322	0.551	0.648	0.474	0.470	0.645	0.548
	T_6	0.206	0.763	0.446	0.867	0.202	0.410	0.500	0.498	0.540	0.536	0.498	0.493

TABLE 6 (continued)

1	2	3	4	5	6	7	8	9	10	11	12	13	14
PO-HAn complex	$l(a\text{-}b)$	1.294	1.368	1.382	1.365	1.332	1.454	1.403	1.395	1.396	1.398	1.394	1.404
	S_0*	0.611	0.452	0.369	0.844	0.379	0.336	0.627	0.672	0.664	0.657	0.679	0.623
	S_1*	0.362	0.257	0.377	0.585	0.431	0.557	0.480	0.713	0.619	0.611	0.712	0.488
	S_2*	0.540	0.399	0.357	0.839	0.369	0.448	0.490	0.495	0.547	0.661	0.497	0.485
	S_3*	0.453	0.338	0.310	0.782	0.319	0.338	0.451	0.710	0.517	0.523	0.709	0.439
	S_4*	0.488	0.360	0.377	0.716	0.417	0.407	0.580	0.448	0.611	0.629	0.453	0.542
	S_5*	0.540	0.394	0.384	0.713	0.433	0.252	0.493	0.493	0.595	0.523	0.505	0.560
	S_6*	0.524	0.392	0.366	0.642	0.403	0.219	0.661	0.421	0.585	0.592	0.421	0.612
	T_1	0.503	0.380	0.752	0.412	0.436	0.461	0.445	0.613	0.526	0.529	0.615	0.437
	T_2	0.417	0.294	0.578	0.457	0.334	0.341	0.613	0.566	0.607	0.619	0.565	0.593
	T_3	0.518	0.436	0.017	0.318	0.369	0.351	0.622	0.666	0.661	0.654	0.673	0.617
	T_4	0.548	0.405	0.853	0.360	0.343	0.467	0.411	0.484	0.595	0.585	0.489	0.466
	T_5	0.574	0.427	0.830	0.366	0.412	0.347	0.502	0.507	0.510	0.502	0.505	0.506
	T_6	0.590	0.436	0.820	0.395	0.457	0.361	0.532	0.479	0.499	0.440	0.469	0.529

[a] Bond length obtained by PPP optimization of geometry.

[b] Bond length from x-ray structures of 5,5'-diphenyl-1,4-phenylene-2,2'-bioxazole (POPOP) [34] and 2,5-diphenyl-1,3,4-thiadiazole [35].

[c] Bond length from x-ray structures of 2-methyl-4-chloromethyl-5-nitrophenyloxazole [37] and 2-(2-hydroxyethyl)-2-thiazoline [38].

[d] $P(S_0)$ and $P(S_1^*)$ are bond orders in the ground and excited S_1* states from INDO/S data.

The oxazole ring of protonated PO–HAn is an electron acceptor in the S_0* and T_1 states ($\sum_i q_i$* = -0.072 and -0.061, respectively) and practically electroneutral in the S_1* state ($\sum_i q_i$* = 0.004). Thus, only the individual electronic properties of the carbon atoms in the rings determine the preferred course of the reaction.

2.5.3. Excitation Localization Numbers. Table 5 contains the calculated excitation localization numbers for the studied molecules. A comparison of the L_i values indicates that the positions with the greatest reactivity seemingly change places in the S_1* and T_1 states: $C_{(2)}$ and $C_{(5)}$ have L_i = 34.8 and 27.3%, respectively, in the S_1* state and L_i = 27.9 and 36.7%, respectively, in the T_1 state. The ratio of L_i indices in the triplet state is more easily tested experimentally because the rate of intercombinational conversion of the triplet state populations of monocyclic molecules is three orders of magnitude greater [19] than optical deactivation of the excess of excitation energy.

The excitation in the PO S_1* state is localized on the benzene ring ($\sum_i L_\mu$ = 87.8%), mainly on $C_{(2')}$ and $C_{(6')}$ (L_μ = 16 and 16.7%, respectively); in the S_2* state, approximately evenly on the heterocycle and benzene, with L_μ = 14.2 and 16.9% for $C_{(2)}$ and $C_{(5)}$, respectively. The excitation in the T_1 state is also localized on the benzene ring ($\sum_i L_\mu$ = 70.7%), including $C_{(4')}$ in the *para* position (L_μ = 14%). Thus, the reaction can be directed differently depending on the spin of the excited state.

Replacement of the oxygen atom by sulfur atom substantially changes the quantities $\sum_i L_\mu$ and L_μ. The excitation in the S_1* state is localized mainly on the thiazole ring ($\sum_i L_\mu$ = 69%), even more so in the T_1 state ($\sum_i L_\mu$ = 84%). Positions 2 and 5 are the most reactive (L_μ = 20.6 and 22.1%, respectively, for the S_1* state and 20.5 and 35%, respectively, for the T_1 state).

Thus, the thiazole ring of PT is more reactive in the triplet state T_1. The quantities $\sum_i L_\mu$ and L_μ alternate in higher lying S_i* and T_j states, as seen in Table 5.

For PO–HAn, the L_μ numbers of the carbon atoms depend strongly on the excited-state spin. For example, atoms $C_{(2)}$, $C_{(4)}$, and $C_{(5)}$ of the oxazole ring are most excited in the S_1* state (L_μ = 22.7, 25.7, and 18%, respectively); atoms $C_{(2')}$, $C_{(4')}$, and $C_{(6')}$ of the benzene ring, in the T_1 state (L_μ = 12.7, 14.9, and 13%, respectively). This correlates with the change in the course of the electrophilic substitution from the azole ring to the *para* position of the benzene ring [9].

2.6. Bond Orders and Molecular Geometry

2.6.1. Comparisons of the Studied Compounds. Table 6 presents the bond lengths and orders for O, PO, and PT that are optimized by the PPP/S-CI method and certain experimental data for the related compounds POPOP (X-ray structure) [34], 2,5-diphenyl-1,3,4-oxadiazole (electron diffraction) [35], and 2,5-diphenyl-1,3,4-thiadiazole (X-ray structure) [36]. In the oxazole ring of PO, the optimized lengths of the single bonds $O_{(1)}$–$C_{(2)}$, $N_{(3)}$–$C_{(4)}$, and $C_{(5)}$–$O_{(1)}$ ($l_{\mu\nu}$ = 1.314, 1.346, and 1.321 Å) are shorter than the experimental values ($l_{\mu\nu}$ = 1.360, 1.384, and 1.378 Å by X-ray diffraction). On the other hand, the double bonds $C_{(2)}$=$N_{(3)}$ and $C_{(4)}$=$C_{(5)}$ are longer ($l_{\mu\nu}$ = 1.323 and 1.377 Å for the optimization and 1.294 and 1.347 Å by X-ray diffraction). In the benzene ring of PO, the optimized bonds are insignificantly longer than the experimental ones but correctly ordered. The X-ray structural data for 2-methyl-4-chloromethyl-5-nitrophenyloxazole [37] produce bond lengths similar to the calculated ones for $C_{(2)}$=$N_{(3)}$ [$l_{\mu\nu}$ = 1.323 (optimized) and 1.320 Å (X-ray structure)] and $C_{(4)}$=$C_{(5)}$ [$l_{\mu\nu}$ = 1.377 (optimized) and 1.360 Å (X-ray structure)].

In the benzene ring of PT, bond lengths similar to the experimental values are obtained. The values for the thiazole ring also agree well. For example, the values for the single bonds $S_{(1)}$–$C_{(2)}$ and $C_{(5)}$–$S_{(1)}$ are $l_{\mu\nu}$ = 1.750 and 1.757 Å, respectively, for optimized PT structure and 1.769 and 1.790 Å, respectively, for the X-ray structure of 2,5-diphenylthiadiazole [36]. Table 6 gives X-ray structural data for the bond lengths in the thiazoline ring of 2-(2-hydroxyethylamino)-2-thiazoline [38]. It is interesting that the bond lengths $C_{(2)}$–S (1.77 Å) and $C_{(5)}$–S (1.79 Å) are similar to the calculated value (1.75 Å) for PT. This can be explained by the comparatively low aromaticity of the thiazole system, in which single and double bonds alternate.

Trends in the distribution of bond orders $p_{\mu\nu}$ in the optimized structures and those calculated from diffraction methods are identical. This indicates that the calculational procedures are highly effective. The calculated UV absorption spectra also support this. The bond strengths redistribute compared with the ground state upon excitation of the molecules. The bond order of single bonds increases. That of double bonds decreases. The increased order of the interring bond $C_{(2)}$–$C_{(1')}$ is especially noticeable: for PO, from $p_{\mu\nu} = 0.295$ in the S_0* state to 0.553 in the S_2* fluorescent state and to 0.423 in the T_1 state. For PT, the change is from 0.329 (S_0) to 0.561 (S_1*) and 0.429 (T_1). This is consistent with an increased interaction of the $\sigma\pi$-electronic subsystems of the rings in the excited states compared with the ground state in which the rings are quasi-autonomous [15].

Experimental proof of the extensive involvement of the interring $C_{(5)}$–$C_{(1')}$ bond in forming the vibronic structure of the absorption and fluorescence bands comes from low-temperature spectra of molecules with the same subsystems [39] and from quantum-chemical calculations [40]. An analysis of the vibronic structure of the fluorescence and phosphorescence bands in the gas phase and solutions shows that the studied molecules in excited states should have coplanar rings. In the ground state, different conformers with rings rotated relative to each other by $\varphi = 24\text{-}45°$ are possible [40]. This provides a basis for using the PPP-CI method [38-40] to calculate the photophysical properties of heterocyclic molecules.

2.6.2. Changes of Bond Orders and Geometry upon Complexation and Protonation. Table 6 presents calculations for PO–HAn taking into account the fact that complexation and protonation change the valence of the nitrogen atom, which also is attacked by the active species. It has been experimentally and theoretically proven [16-23, 37, 38] that the properties of the excited states, the photophysical properties, and the structures that are calculated using quantum-chemical methods correspond with the idealized model of a monomolecular gas [16-23].

The effect of aggregation on the active molecule can in certain instances be modelled by selecting the spectral parameters (ionization potential and electron affinity [37-42]) in terms of the direct and inverse spectroscopic problems. However, this can be done only for those atoms that are primarily affected by the solvent (for example, the valence change of the nitrogen atom upon protonation of the unshared electron pair in acid solutions [16] or on a catalyst surface owing to interaction with its acid centers [37]). Obviously the changes occur mainly in the heterocycle whereas they are insignificant in the benzene ring. On going from PO to PO–HAn, the order of the interring C–C bond increases from 0.295 to 0.336 (ground state) or to 0.557 (S_1*) and 0.445 (T_1). Thus, the $\sigma\pi$-conjugation in the ground state of PO–HAn is stronger than in that of PO. Changes in the charges and bond orders of one of the subsystems predictably changes its geometry and the nature of the vibronic interaction of the atomic groups in the rings in the excited states. Quantum-chemical calculations of the UV absorption spectra of PO and PO–HAn are consistent with this (Fig. 4).

CONCLUSION

A regular bathochromic shift of the UV absorption, the 0–0 transition, and fluorescence bands is observed in the studied series of heterocyclic molecules upon increasing the number of chemical bonds and rings (i.e., on going from mono- to bicyclic systems), replacing an atom with a smaller atomic number by one with a larger number, and upon complexation or protonation of the nitrogen atom. This is due to the changes in the quantum energy and a redistribution of electron density on the atoms and bonds that are caused by structural transformations.

The observed luminescence of PO, PT, and their protonated complexes is determined by the electron-density distribution on the ring atoms in a long-lived triplet state. The changes induced by protonation of the nitrogen atom that occur in the frequency of the 0–0 transition and the localized vibronic interactions of bonded groups in the rings, which are mainly subject to electron excitation, are due primarily to a change in the electronic and steric structure of the heterocycle of the azoles.

REFERENCES

1. N. A. Borisevich, *Excited States of Complicated Molecules in the Gas Phase* [in Russian], Nauka i Tekhnika, Minsk (1967).
2. B. M. Krasovitskii and B. M. Bolotin, *Organic Luminophores* [in Russian], Khimiya, Moscow (1984).
3. F. F. Vol'kenshtein, *Electron Processes on Semiconductor Surfaces During Chemisorption* [in Russian], Nauka, Moscow (1987).
4. G. E. Dobretsov, *Fluorescence Probes in Cell, Membrane, and Lipoprotein Research* [in Russian], Nauka, Moscow (1989).
5. A. N. Terenin, *Dye Photonics* [in Russian], Nauka, Leningrad (1967).
6. Y. J. D. Berlman, *The Fluorescence Spectra of Aromatic Molecules*, Academic Press, New York (1971).
7. T. Clark, *A Handbook of Computational Chemistry. A Practical Guide to Chemical Structure and Energy Calculations*, John Wiley and Sons, New York (1985).
8. A. I. Kitaigorodskii, P. M. Zorkii, and V. K. Bel'skii, *Structure of Organic and Organometallic Molecules: A Bibliography of References from 1929-1970* [in Russian], Nauka, Moscow (1984).
9. L. I. Belen'kii, M. A. Cheskis, V. P. Zvolinskii, and A. E. Obukhov, *Khim. Geterotsikl. Soedin.*, No. 6, 826 (1986).
10. A. E. Obukhov, L. Sh. Afanasiadi, L. D. Patsenker, and V. M. Shershukov, *Khim. Geterotsikl. Soedin.*, No. 10, 1414 (1989).
11. L. I. Belen'kii and M. A. Cheskis, *Khim. Geterotsikl. Soedin.*, No. 7, 881 (1984).
12. L. I. Belen'kii, G. P. Gromova, M. A. Cheskis, and Yu. I. Gol'dfarb, *Chem. Scripta*, **25**, 295 (1985).
13. L. I. Belen'kii, M. A. Cheskis, and M. A. Ryashentseva, *Khim. Geterotsikl. Soedin.*, No. 6, 822 (1986).
14. L. I. Belen'kii, S. I. Luiksaar, I. S. Poddubnyi, and M. M. Krayushkin, *Izv. Akad. Nauk, Ser. Khim.*, No. 11, 2309 (1998).
15. A. E. Obukhov, *Izv. Ross. Akad. Nauk, Ser. Fiz.*, **56**, 210 (1992).
16. A. E. Obukhov, *Kvantovaya Elektron. (Moscow)*, **20**, 863 (1993).
17. A. E. Obukhov, *Zh. Fiz. Khim.*, **69**, 1015 (1995).
18. A. E. Obukhov, *Laser Phys.*, **7**, 1102 (1997).
19. A. E. Obukhov and L. I. Belen'kii, *Khim. Geterotsikl. Soedin.*, No. 9, 1181 (1998).
20. D. N. Shigorin, G. A. Val'kova, G. A. Gastilovich, V. A. Godik, G. G. Konoplev, M. A. Pak, A. N. Rodionov, and N. S. Strokach, *Electronically Excited States of Polyatomic Molecules and Their Deactivation Processes* [in Russian], Nauka, Moscow (1993).
21. A. N. Rubinov and V. I. Tomin, *Progress in Science and Technology. Radiotechnology Series*, Vol. 9 [in Russian], Moscow (1976), p. 5.
22. B. I. Stepanov (ed.), "Optical laser calculations," in: *Science and Technology*, Vol. 1 [in Russian], Minsk (1966).
23. J. Hinze and H. H. Jaffe, *J. Phys. Chem.*, **56**, 1501 (1963).
24. A. V. Luzanov, *Usp. Khim.*, **49**, 2086 (1980).
25. N. Mataga and K. Nishimoto, *Z. Phys. Chem.*, **13**, 140 (1957).
26. G. A. Shchembelov, Yu. A. Ustynyuk, V. M. Mamaev, and I. P. Gloriozov, *Quantum-Chemical Methods of Calculating Molecules* [in Russian], Khimiya, Moscow (1980).
27. S. S. Batsanov, *Chemical Bond Cleavage Energy. Ionization Potentials and Electron Affinity* [in Russian], Nauka, Moscow (1974).
28. J. N. Murrell, S. F. A. Kettle, and J. M. Tedder, *The Chemical Bond*, John Wiley and Sons, New York (1978).
29. M. J. S. Dewar and S. D. Worley, *J. Chem. Phys.*, **50**, 654 (1969).
30. F. H. Allen, O. Kennard, D. G. Watson, L. Brammer, A. G. Orpen, and R. Taylor, *J. Chem. Soc., Perkin Trans 2*, No. 12, 1 (1987).
31. L. I. Belen'kii, V. S. Bogdanov, I. A. Abronin, G. P. Gromova, M.A. Cheskis, and R. Z. Zakharyan, *Chem. Scripta*, **25**, 266 (1985).

32. L. M. Sverdlov, *Vibrational Spectra of Polyatomic Molecules* [in Russian], Nauka, Moscow (1970).
33. A. E. Obukhov, *Fiz. Mysl' Ross.*, **1**, 6 (1996).
34. I. Ambats and R. E. March, *Acta Crystallogr.*, **19**, 942 (1965).
35. N. I. Popik, M. V. Shablygin, L. V. Vilkov, A. S. Semenova, and T. V. Kravchenko, *Vysokomol. Soed., Ser. B*, **25**, 38 (1983).
36. Z. V. Zvonkova and A. N. Khvatkina, *Kristallografiya*, **10**, 734 (1965).
37. V. Albano, P. L. Bellon, F. Pompa, and V. Scatturin, *Ric. Sci.*, **33**, 1143 (1963).
38. R. A. L. Miller, J. M. Robertson, G. A. Sim, R. C. Clapp, L. Long, and T. Hasselstrom, *Nature*, **202**, 287 (1964).
39. L. I. Belen'kii, I. A. Vasil'eva, M. D. Galanin, A. N. Nikitina, and Z. A. Chizhikova, *Opt. Spektrosk.*, **68**, 801 (1990).
40. K. Gustav and C. Seydenschwarz, *Chem. Phys. Lett.*, **109**, 156 (1984).